RevMexAA (Serie de Conferencias), **10**, 163–168 (2001)

THE MULTIPUPIL FIBER SPECTROSCOPY OF THE CRAB-PULSAR NEIGHBOURHOOD

S. V. Zharikov,[1] Yu. A. Shibanov,[2] A. B. Koptsevich,[2] V. L. Afanasév[3] and S. N. Dodonov[3]

RESUMEN

Presentamos la espectroscopía óptica resuelta espacialmente del entorno de $12'' \times 24''$ del pulsar del Cangrejo en el intervalo $\lambda\lambda 4600-5700$A hecha con el Espectrógrafo de Fibras Multipupila del telescopio de 6 m del *SAO RAS*. Los espectros exhiben líneas de [O III] fuertes y líneas de emisión H_β y He II débiles con desplazamientos e intensidades que varían con la posición en el campo. Esto indica la presencia de una estructura tipo cono centrada en la posición del pulsar que rota y está orientada a lo largo del eje de simetría de la "nebulosidad" compacta toroidal del pulsar observada en el contínuo óptico y en rayos X suaves. Esto puede ser explicado mediante la rotación de material emisor en el plano ecuatorial, girando en sentido anti–horario con respecto al eje de rotación del pulsar, a una velocidad $\sim$ 2000–3000 km/s y a una distancia de varios miles de UA del pulsar.

ABSTRACT

We present the spatially resolved optical spectroscopy of the $12'' \times 24''$ Crab pulsar neighbourhood in the range $\lambda\lambda 4600-5700$ Å made with the Multipupil Fiber Spectrograph at the 6 m telescope of the SAO RAS. The spectra exhibit blue– and red–shifted strong [O III] and weaker H_β and He II emission lines with the shifts and intensities varying with the position in the field. They hint the presence of a cone–like rotating structure centered at the pulsar position and oriented along the symmetry axis of the compact, torus–like pulsar nebula seen in optical continuum and soft X–rays. The kinematic structure is most likely associated with the pulsar nebula. If so, the compact nebular rotates counter–clockwise with respect to its symmetry axis, or the pulsar spin axis, and the estimated rotational velocity within cylindrical radii of several thousand AU from the pulsar is $\sim$ 2000–3000 km/s.

Key Words: **ISM: INDIVIDUAL: CRAB NEBULA — ISM: SUPERNOVA REMNANTS — TECHNIQUES: SPECTROSCOPIC**

1. INTRODUCTION

The Crab nebula is a well–known, young (945 yrs) type II supernova remnant of $\sim 6' \times 4'$ angular size and with the pulsar near its center. Located 200 pc from the Galactic plane at the distance about 2 kpc from the Earth, the Crab nebula has been extensively studied at all wavelengths from radio to gamma–rays. Observations show that kinematics and morphology of the remnant shell on the whole, and the large–scale bipolar asymmetry in the abundance, geometry, and velocity distribution of bright filaments inside the nebula are associated with the activity of the young and energetic Crab pulsar (e.g., Clark et al. 1983; Lawrence et al. 1995; Hester et al. 1995, 1996; Blaer et al. 1997 and refs. therein). Although it is generally clear that the nebula is mainly powered by the wind of relativistic particles from the pulsar, very little has been known of the details of the structure of the wind, and of the mechanisms of its acceleration and interaction with the ambient matter. High spatial resolution, multiwavelength observations of a compact, $\lesssim 1'$, central region around the

[1]Observatorio Astronómico Nacional, Instituto de Astronomía, Universidad Nacional Autónoma de México, Ensenada, B. C., México
[2]Ioffe Physical Technical Institute
[3]Special Astrophysical Observatory of the Russian Academy of Sciences

The Seventh Texas-México Conference on Astrophysics: Flows, Blows and Glows (Austin, Texas, 6-8 April 2000)
Editors: William H. Lee and Silvia Torres-Peimbert

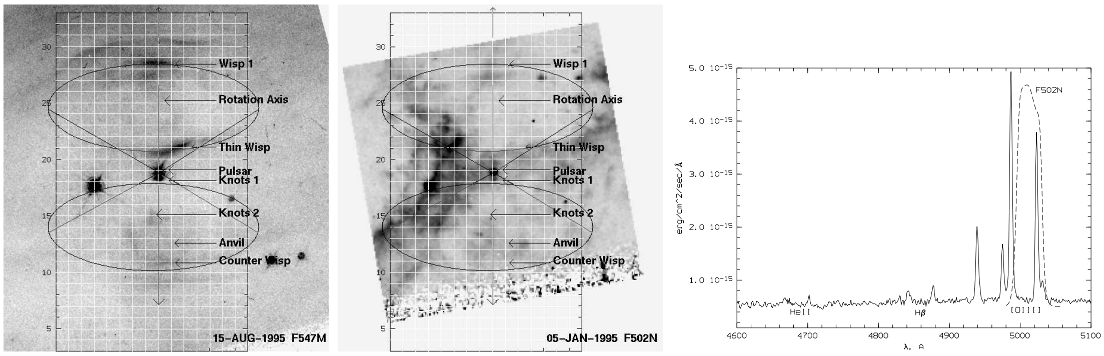

Fig. 1. *Left and Middle:* Images of the Crab pulsar compact nebula obtained with the HST by Hester et al. (1995; 1996) in the F547M band, which is free of strong emission lines from the nebula, and in the narrow F502N band containing a strong [O III] emission (see *the right panel*). We use the data retrieved from the HST archive and follow known notations (Hester et al. 1995) of the nebula structures that are formed by the pulsar relativistic wind in the optical continuum. The white grid shows the $12'' \times 24''$ area that was covered in our observations; its $(0.75'')^2$ meshes are the MPFS spatial elements. *Right:* The spectrum taken from the region containing the pulsar, which is marked by the square in *the left panel* of Fig 2. It exhibits the red and blue shifted [O III], H_β, and He II emission lines originating in the nebula. The pulsar spectrum is almost flat and has no features in this range (see, e.g. Nasuti et al. 1996). The F502N throughput shown by dashed line demonstrates that the structures seen in the F502N image (*Middle*), but lacking in the continuum image (*Left*), are mainly caused by the redshifted component of [O III].

pulsar hold the most promise to resolve these problems. Indeed, the images of the Crab–pulsar vicinity obtained recently with subarcsecond spatial resolution in optical continuum with the HST and in soft X–rays with the ROSAT (Hester et al. 1995) and with the Chandra (Weisskopf et al. 2000) observatories, revealed a fascinating axially symmetric picture of the compact pulsar nebula with equatorial torus-like structures and polar jets probably oriented along the presumed pulsar spin axis. It is important that the optical and X–ray images are mutually complementary. Spatial resolved spectroscopy, which provides 3D (two space+radial velocity) investigations of spatial and kinematic structures, would be the natural next step in the studies of the compact pulsar nebula.

We report two–dimensional optical spectroscopy of the Crab pulsar neighbourhood obtained with the Multipupil Fiber Spectrograph (MPFS) at the 6 m telescope of the Special Astrophysical Observatory (Nizhnij Arkhyz, Russia). A compact, axially–symmetric rotating structure centered at the pulsar position has been detected for the first time in emission lines with Doppler shifts up to ± 1500 km/sec. We discuss its possible association with the axially–symmetric pulsar nebula seen in the optical continuum and in X–rays.

2. OBSERVATIONS AND DATA REDUCTION.

The observations were carried out on 1999 November 11 with seeing of about $1.7''$, in the spectral range $\lambda\lambda 4600 - 5700$ Å with the dispersion 1.35/px. The MPFS spatial element size was $0.75'' \times 0.75''$, and the FOV was 16×16 spatial elements, or $12'' \times 12''$ (see Afanasiev et al. 1996 for technical details of the MPFS). A region (see images in Fig. 1) of the size $12'' \times 24''$, or $\sim 0.1 \times 0.2$ pc for the pulsar distance of 2 kpc, centered at the pulsar position was covered by three spatially overlapping exposures. The main axis of the region was chosen along the cylindrical symmetry axis of the compact pulsar nebula. A schematic representation of the cone–like structure of the nebula and its components in the optical is indicated in Fig. 1 following Hester et al. 1995. Standard data reduction was performed including the "bias" substraction, flat–fielding, and removal of cosmic rays and correction for geometric distortions. We obtained a total of 768 spectra related to the different spatial elements of the region. Data analysis showed that the spectra from the first line of the MPFS matrix at each exposure were of a bad quality for unknown reasons. Since overlapped images were obtained, the corrupted line in one of the images was replaced by a good one from another. As a result, our final analysis is based on 720 good–quality spatially resolved spectra. The spectrum of HZ44 was used for the spectrophotometric calibration. The MPFS data allow us to construct images of the region in any wave band within the observed

The Seventh Texas-México Conference on Astrophysics: Flows, Blows and Glows (Austin, Texas, 6-8 April 2000)
Editors: William H. Lee and Silvia Torres-Peimbert

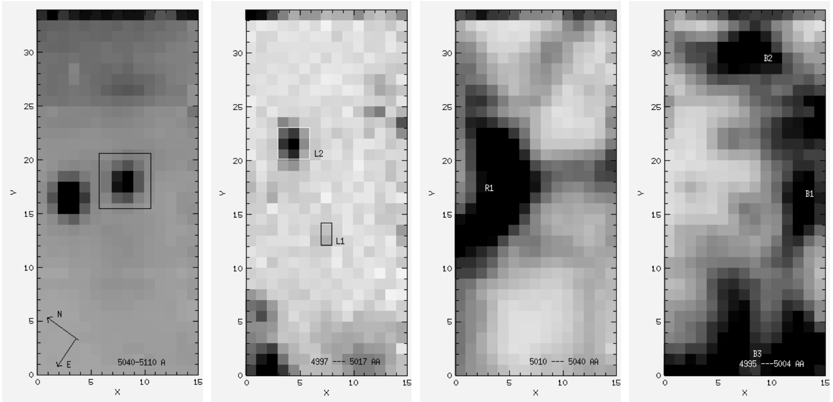

Fig. 2. The images of the Crab pulsar field constructed from the MPFS data in different wavebands which filter the emission in the continuum, in the low shifted, high red–shifted, and high blue–shifted [O III] lines, *from left to right*, respectively. The chosen band–passes and the velocity estimates are given in the text. The pixel size is $(0.75'')^2$. Axis of the pulsar nebula symmetry, supposed to be the pulsar spin axis, is oriented vertically, as in Fig. 1.

spectral range.

3. RESULTS AND DISCUSSION

The spectra exhibit strong, $S/N \sim 20-50$, blue– and red–shifted [O III] $\lambda\lambda 5007, 4959$Åemission lines, as well as much weaker H_β $\lambda 4861$ Å and He II $\lambda 4686$ Å emission. The Doppler shifts of their centroids yield the motion of the emitting matter with velocities up to $\pm$ 1500 km/s. A typical spectrum of a spatial element containing the pulsar is shown in the right panel of Fig. 1. The intensities of the components and their Doppler shifts vary with the spatial coordinate.

To study the spatial distribution of the emission and kinematics of the region we constructed the images in four spectral bands: (i) in the continuum in the $\lambda\lambda 5040-5100$ Å range; (ii) in the low velocity ($\lesssim |\pm 600|$ km/s) component of [O III] within $\lambda\lambda 4997-5014$ Å; (iii) in the high velocity ($\gtrsim +600$ km/s) red–shifted component of [O III] within $\lambda\lambda 5010-5040$ Å; and (iv) in the high velocity ($\lesssim -600$ km/s) blue–shifted component of [O III] within $\lambda\lambda 4985-5004$ Å (see Fig. 2). In cases (ii)–(iv) the continuum was subtracted to remove the background and to clear the kinematic structure seen only in the emission lines.

The pulsar and nearby star leftwards of the pulsar are bright and clearly seen in the continuum (Fig. 2, left panel). We can identify also the Wisp 1 and the Anvil structures marked in Fig. 1 above and below of the pulsar's position. They are smoothed in our image due to lower spatial resolution in comparison to the HST/WFPC2 ($\sim 1.7''$ *vs* $\sim 0.1''$). In the low velocity ($\lesssim |\pm 600|$ km/s) [O III] image (2d panel from the left in Fig. 2) we find a number of structures of various brightnesses and geometry. Some of them are marked by boxes with L–number. The structure L1 is rather faint. It is located in the Anvil and possibly associated with the relatively bright HST source, Knot 2. It is detected as a faint object in our continuum image also. The Knot 2 is projected at the south–east polar jet from the pulsar clearly seen in X–rays. It may be related to a shock–wave or a plasma instability inside the jet. If L1 is indeed Knot 2, its line–of–sight velocity component estimated from the spectra of the respective spatial elements is about 200 km/s. Another low velocity structure L2 is associated with the bright compact region in the F502N image and has the velocity of about 600 km/s.

The images constructed in the narrow spectral bands centered at the high velocity red– and blue–shifted components of [O III] (3d and 4th panels from the left in Fig. 2, respectively) are markedly different from each other and from the two previous images. They hint for the first time at the presence of an axially symmetrical, cone–like rotating structure centered at the pulsar position and oriented along the nebula symmetry axis: in close vicinity of the pulsar the red–shifted emission is concentrated mainly north–east, while the blue component is south–west of the pulsar position, or leftward and rightward of the symmetry axis, respectively. The cone–like structure is most clearly seen in the [O III] red–shifted component. In the blue–shifted component it is patchy and less certain. Our analysis shows that the highly red–shifted emission of [O III] can be decomposed into two main components with velocities $\sim 900-1000$ km/s and $\sim 1100-1350$ km/s. Their brightnesses and velocities vary with the position in the image. As a rule, the spectral profiles of the blue–shifted emission are simpler and contain only one velocity component. Only a few of spatial elements exhibit a multi–velocity structure of the blue–shifted [O III] emission. The average velocity of the high blue–shifted component is in the range $\sim 1000-1300$ km/s which is quite symmetrical to the range of the high red–shifted components $\sim 900-1350$ km/s. This confirms that both components originate in the same rotating structure. Note, our image in the red–shifted component of [O III] is consistent with the HST image obtained in the narrow F502N filter (middle panel in Fig. 1). It is explained by coincidence of the band-pass of this filter with the mean position of the red component in the spectrum, as demonstrated in the right panel of Fig. 1.

In our observations, we have not found any evidence for relativistic, $\sim 0.5c$, outward motion of the wisp structures reported by Hester et al. 1998 based upon a set of the HST images in the continuum (F547M) obtained within a one week time scale. These unstable and short–lived structures were either absent at the time of our observations or they are too small, $\sim 0.3''$ and faint to be registered with our spatial resolution, or they do not emit in strong lines. The maximum velocity we registered is about 1450 km/s. We should note that the kinematic structure of the pulsar neighborhood in [O III] is reproduced also in H_β and He II emission lines but with lower signal–to–noise ratio. For instance, the mean ratio of the flux in [O III] to that in H_β is about 14.

There are two possible interpretations of our observations: (1) we see a fine kinematic structure of a thin filament in an outer region of the Crab nebula by chance projected at the pulsar field; (2) the observed structure is associated with the internal part of the compact pulsar nebula.

Although basing on our observations of a small, $12'' \times 24''$, region and available observations of the pulsar field in different wave bands we cannot completely rule out the first hypothesis, there are several arguments in favor of the second one. The main one is the similar axial symmetry of the observed kinematic picture and the morphology of the pulsar field seen in the optical continuum and X–rays. Additionally, even within the rather moderate spatial resolution of our observations, some details of the kinematic picture are associated with characteristic details of the spatial structure (Knot 2 in the X–ray jet, Anvil, Wisp 1 forming an optical halo coinciding with the X–ray ring/torus, etc.) obtained at much higher resolution in the continuum. The cone–like geometry of the kinematic structure is in general agreement with the qualitative picture of the pulsar–wind zone suggested by Hester et al. 1995 and shown in Fig. 1. If so, taking into account that the symmetry axis lies about 30^o out of the celestial plane (e.g., Weisskopf et al. 2000), we see partially ionized gas rotating counter–clockwise with respect to the pulsar spin axis with a velocity $\sim 2000-3000$ km/s within cylindrical radii of several thousand AU from the neutron star. It is natural to assume that the pulsar spins in the same direction also and a part of the angular momentum of the strongly magnetized neutron star is transferred with the relativistic wind into the ambient nebula matter. In accordance with the cone–like structure in Fig. 2, the rotating equatorial wind zone extends up to $\sim \pm 60^o$ of the pulsar latitude with respect to its spin axis.

We plan to extend our spatially resolved spectroscopy to a larger area around the pulsar to confirm or reject the inferred kinematic structure of the compact Crab-pulsar nebula.

The work was supported by the INTAS 96-0542, RFBR 99-02-18099, and CONACyT N25454-A grants.

REFERENCES

Afanasiev, V. L., Dodonov, S. N., Drabek, S. V. & Vlasyuk, V. V. 1996, MPFS Manual (Nizjnij Arkhyz: SAO)
Blaer, W. P., Davidson, K., Fesen, R. A., Uomoto, A., MacAlpine, G. & Henry, R. B. C. 1997, ApJS, 109, 473
Clark, D. H., Murdin, P., Wood, R., Gilmozzi, R., Danziger, J. & Furr, A. W. 1983, MNRAS, 204, 415
Hester, J. 1998, in: Neutron Stars and Pulsars, eds. N. Shibazaki, N. Kawai, S. Shibata & T. Kifune, Univ. Acad. Press, Inc., Tokyo, Japan, p. 431
Hester, J. J. et al. 1995, ApJ, 448, 240
Hester, J. J. et al. 1996, ApJ, 456, 225
Lawrence S. S. et al. 1995, AJ, 109, 2635
Nasuti, F. P., Mignani, R., Caraveo, P. A., Bignami, G. F. 1996, A&A, 314, 849
Weisskopf, M. C. et al. 2000, ApJ, 536, L81

The Seventh Texas-México Conference on Astrophysics: Flows, Blows and Glows (Austin, Texas, 6-8 April 2000)
Editors: William H. Lee and Silvia Torres-Peimbert

S. Zharikov: O. A. N. IA–UNAM, Ensenada, B. C. 22860, México, zhar@astrosen.unam.mx.
Y. Shibanov and A. Koptsevich: Ioffe Phys. Tech. Inst., Politekhnicheskaya 26, St. Petersburg, 194021, Russia.
V. Afanasév and S. Dodonov: Spec. Astro. Obs. of RAS, Karachai–Cherkessia, Nizhnij Arkhyz, 357147, Russia.

The Seventh Texas-México Conference on Astrophysics: Flows, Blows and Glows (Austin, Texas, 6-8 April 2000)
Editors: William H. Lee and Silvia Torres-Peimbert

RevMexAA (Serie de Conferencias), **10**, 168–175 (2001)

AXISYMMETRIC ROTATOR MODELS AS PULSARS: ABJECT FAILURE

F. C. Michel and I. A. Smith

Space Physics and Astronomy, Rice University, Houston, TX, USA

RESUMEN

El bien conocido modelo de Goldreich & Julian (1969) postuló que aún una estrella de neutrones en rotación con un momento de campo magnético dipolar alineado sería un pulsar activo. Aunque se sospechó desde 1980 que este modelo no podría funcionar como se propuso, hemos visto el resurgimiento de modelos que no perciben los problemas básicos subyacentes. A menos que esos modelos identifiquen explícitamente el vicio de la falla de los modelos GJ, no se les debe dedicar tanto esfuerzo teórico.

ABSTRACT

The well–known Goldreich & Julian (1969) model postulated that even a rotating neutron star with an aligned magnetic dipole moment would be an active pulsar. Although it was suspected as long ago as 1980 that this model could not work as posed, we have now seen a resurgence of models that do not realize the basic underlying problems. Unless such models can explicitly identify where the failure of the GJ model is vitiated, they may not be a useful place to devote so much theoretical effort.

Key Words: **MAGNETOHYDRODYAMICS — PLASMAS — PULSARS: GENERAL — STARS: NEUTRON**

1. INTRODUCTION

Although Goldreich & Julian (1969) are usually credited with calculating the “Goldreich and Julian charge density” around rotating conductors having an aligned magnetic dipole moment, this was apparently first estimated for stars in general by Davis, (1947; 1948). Later Hones & Bergeson (1965: HB) extended this treatment for the more general case of a non–aligned dipole moment, here applied to planetary magnetospheres. However, except for the parameter space (explicit values of magnetic moment, stellar radius, and rotation rate), these estimates are as valid for planets as for pulsars. Indeed, the application to, say, the Earth’s magnetosphere is even more plausible than to pulsars, since the magnetosphere is known to be abundantly full of plasma to provide the (negligible) space–charge separation about the Earth: the Hones and Bergeson (HB) charge density. Accordingly, HB imposed the so–called exact MHD condition which assumes that the magnetic field lines are perfect conductors along these field lines and perfect insulators across them. Consequently, the magnetic field lines become electrical equipotentials, with the value of each potential being determined at the stellar/planetary surface. Given this potential, one can take the Laplacian to obtain the required charge separation. Since the magnetic field lines then effectively extend the same electric fields as inside the star, the magnetosphere should then rigidly corotate with the star. (In the case of the Earth’s magnetosphere, the interaction with the external solar wind is the dominatant perturbation, which largely overwhelms the effects of the Earth’s rotation.)

Goldreich and Julian proposed exactly the same electrodynamics, simplified to the aligned case, but to the case of neutron stars. Neutron stars, unlike planets, are not expected to maintain quasi–neutral plasma in their magnetospheres owing to the intense gravitational field. Nevertheless, they too assumed ideal MHD, which then required the neutron star to be surrounded by space charge (we try to make the distinction between charge–separation, which can always be obtained at any given point in space given sufficient *local* conduction charges, and space–charge, which can only be obtained by transport of charge from some source *elsewhere*). Indeed, GJ explicitly proposed that this space–charge comes from the neutron star surface (pulled off by the